

# Effect of microwave sintering on the microstructure and electric properties of (Zn,Mg)TiO<sub>3</sub>-based multilayer ceramic capacitors

Ying-Chieh Lee\*, Yu-Yuan Yeh, Pei-Rong Tsai

*Department of Materials Engineering, National Pingtung University of Science & Technology, Pingtung 91201, Taiwan*

Received 24 August 2011; received in revised form 19 December 2011; accepted 22 December 2011

Available online 18 January 2012

## Abstract

In this study, the effects of microwave sintering on the sintering behaviour, microstructure and silver diffusion of (Zn,Mg)TiO<sub>3</sub>-based multilayer ceramic capacitors (ZMT MLCCs) with pure silver electrodes were investigated. The energy dispersive spectroscopy results showed that the silver ions diffused into the dielectric layer significantly when the ZMT MLCC was sintered with conventional processing at 900 °C. However, sintering of ZMT MLCC at 900 °C using microwave processing was found to effectively suppress silver ion diffusion into the dielectric layer. The concentration of silver ions was identified by wavelength dispersive spectroscopy, which showed that the Ag ion concentrations for conventional and microwave sintering are approximately 1.0 at.% and below 0.4 at.%, respectively. The observed difference may be due to different kinetics between conventional and microwave sintering.

© 2011 Elsevier Ltd. All rights reserved.

**Keywords:** Silver diffusion; MLCC; Dielectric layer; Microwave sintering; Insulation resistance

## 1. Introduction

Miniaturisation, performance, and cost savings are the major drivers in the manufacture of multilayer ceramic capacitors (MLCCs), although many manufacturers have switched over from Ag–Pd electrodes to base metal electrode systems.<sup>1,2</sup> Pure silver inner electrodes have a cost advantage when compared to base metal systems, and silver is also the most conductive element, facilitating lower ESR (equivalent series resistance) and higher frequency requirements. However, multilayer ceramic capacitors are one of the most widely used discrete electronic components, playing a critical role in the electronics industry. The use of silver rather than pure palladium as the conductor for MLCCs is one way to reduce costs.<sup>3–5</sup> Therefore, due to the development of many low-sintering ceramic formulations, Ag pastes have been widely used as internal electrodes in the metal–ceramic cofiring step during the fabrication of these multilayer ceramic devices.<sup>6</sup> However, during the cofiring of the ceramic layers and silver inner electrodes, the potential for chemical reactions and inter-diffusion at the interfaces

must be considered along with their influence on the cofiring behaviour of MLCCs. The interaction and inter-diffusion may change the sintering behaviour and final properties of the MLCCs.<sup>7,8</sup> It is well known that zinc titanates (ZnTiO<sub>3</sub>) can be sintered at 1100 °C without the use of sintering aids.<sup>9,10</sup> When a sintering aid is added, it can be sintered at temperatures below 900 °C.<sup>9–11</sup> ZnTiO<sub>3</sub> has a perovskite-type oxide structure and should be useful as a microwave resonator material.<sup>10</sup> ZnTiO<sub>3</sub> material has a permittivity ( $\epsilon_r$ ) of 19, a  $Q$  value of 3000 at 10 GHz, and a temperature coefficient of resonant frequency ( $\tau_f$ ) of  $-55$  ppm/°C.<sup>11,12</sup>

Microwave sintering is a method of internal self-heating by absorption of microwave power. Therefore, comparing the internal microwave sintering is possible with external sintering by thermal conduction or radiation. When this method is utilised in the processing of ceramics, the material is expected to display fine grain, uniformity and high densification. Additionally, the electrical and mechanical properties can be improved.<sup>13</sup>

It is well known that silver migration into ceramics in the cofiring process of low sintering temperature MLCCs significantly influences the reliability and dielectric characteristics.<sup>14–18</sup> In a previous study,<sup>19</sup> the effect of heating rates and two-step sintering on the diffusion of Ag into the ZMT dielectric were investigated. It was found that two-step

\* Corresponding author. Tel.: +886 8 7703202, fax: +886 8 7740552.  
E-mail address: [YCLee@mail.npust.edu.tw](mailto:YCLee@mail.npust.edu.tw) (Y.-C. Lee).

sintering can effectively prevent the Ag ions from diffusing into the dielectric layer. However, the influence of microwave sintering on the Ag diffusion of MLCCs was not investigated. In this paper, the effects of microwave sintering on the sintering behaviour, microstructure and silver diffusion of ZMT MLCCs with pure silver electrodes were investigated.

## 2. Experimental

### 2.1. Preparation of the ZMT powders

ZMT powders were synthesised by conventional solid-state methods from individual high-purity oxide powders: ZnO (99.8% Umicore Zinc Chemicals, France), TiO<sub>2</sub> (99.9% Showa Denko Inc., Japan) and MgO (99% Pharmacie Central Inc., France). They were mixed and ground in deionised water with 2 mm zirconia beads for 24 h; the mean particle size ( $D_{50}$ ) of the milled powder was approximately 0.35  $\mu\text{m}$ . The powders were calcined in air at 900 °C for 5 h after ball milling. 3ZnO–B<sub>2</sub>O<sub>3</sub> (ZnBO) glass with 1  $\mu\text{m}$  particle size was chosen as a sintering aid and added to constitute 1.0 wt% of the powder. The calcined powders were then milled again for 6 h. The mean particle size was measured to be approximately 0.5  $\mu\text{m}$ .

### 2.2. Fabrication of multilayered ZMT capacitors

In this experiment, the MLCCs consisted of ten active layers with an overall size of 2.0 mm  $\times$  1.25 mm  $\times$  0.85 mm, with a distance of 17  $\mu\text{m}$  between the internal electrodes. The ZMT powders were mixed with resin (polyvinyl butyral), plasticiser (butyl benzyl phthalate) and solvent (toluene and ethanol). The resultant slurry was tape-casted to a green sheet with 30  $\mu\text{m}$  thickness using the doctor-blade method.

A silver paste composed of silver particles, binder and solvent was prepared for screen printing. A silver powder (Ag C200ED, Ferro Co., USA) with average particle size of 1.1  $\mu\text{m}$  was used. The powder/organic vehicle ratio was 90/10 by weight. The pastes were prepared and homogenised on a standard three-roller mill. The paste consisted of 60% solid material and had a viscosity of 25 Pa s by 10 rpm.

Ag paste was printed as an inner electrode onto the green sheet. These printed sheets were stacked, pressed at 60 °C under a pressure of  $5.2 \times 10^7$  Pa and cut into chips. The laminated green chip was sintered in a microwave oven after binder burn-out (320 °C). The samples were sintered in air by microwave processing, ramping at 15 °C/min. The temperature of the sample was monitored with a type-R thermocouple shielded with platinum foil and grounded to the inner metallic wall of the microwave furnace. The samples were sintered at various temperatures from 800 °C to 900 °C, held for 60 min at the peak temperature. Comparative conventional sintering was carried out in a regular resistance furnace at the same heating rate and holding time. Samples were microwave sintered using a single-mode microwave furnace with a cavity of 37 cm  $\times$  34.5 cm  $\times$  33.5 cm. The microwave sintering experiments were conducted in a 2.4 kW, 2.45 GHz. The samples were

encased in a microwave susceptor (SiC) located in a thermal insulation package in the microwave chamber.

### 2.3. Measurements

The sintering shrinkage of the ZMT dielectrics and silver powders was measured at a heating rate of 5 °C/min in air by a thermo-mechanical analyser (TMA, Netzsch DIL 402C, Germany). Both ZMT dielectrics and silver powders were pressed to form a disc with 10 mm diameter and 1 mm thickness. The capacitance and dissipation factor were measured at 1 MHz and 23 °C by an impedance analyser (HP 4278A, Palo Alto, CA). Microstructural observation of the sintered MLCC was performed with a scanning electron microscopy (SEM, Jeol, JXA-8900R Japan) equipped with wavelength-dispersive spectrometer (WDS). In each test, five samples were analysed, and 6 points were analysed on each sample for a total of 30 points to ensure WDS reliability and reduce errors. The insulation resistance was measured with a high resistance meter (HP 4140A, Palo Alto, CA) at a dc voltage of 50 V for 1 min. Sintering temperature is measured using an optical pyrometer (President Honor industries Co., Ltd., Taiwan) focused directly onto the samples. The model of optical pyrometer is SH60 which can be applied at 600–1200 °C. The pyrometer is directly connected to the controller and does not influence or interfere with the microwave field distribution within the cavity. However, the traditional metal thermocouples can interfere with the microwave field within the cavity preventing accurate measurements from being made. The optical pyrometer was calibrated at several temperature points using a type B PtRh thermocouple placed in contact with the samples.

## 3. Results and discussion

### 3.1. Effect of microwave sintering on the density and microstructure of ZMT dielectric

Fig. 1 shows the bulk density of the ZMT ceramic pellets from each sintering process as a function of the sintering temperature. The density of ZMT ceramics sintered at different temperatures depends on the heating mode. For the ZMT ceramics sintered by

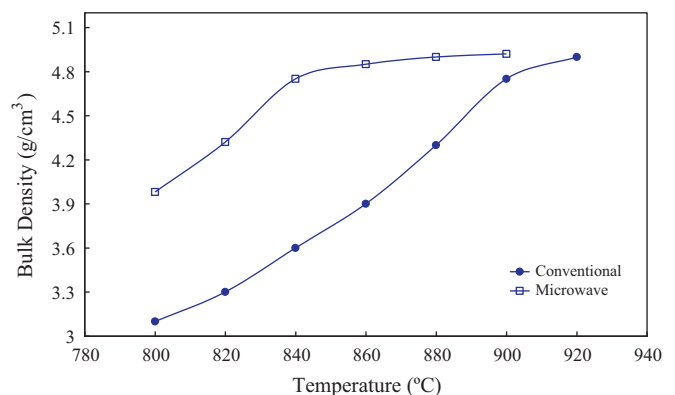


Fig. 1. The bulk density of ZMT ceramics produced by both sintering methods as a function of the sintering temperature.

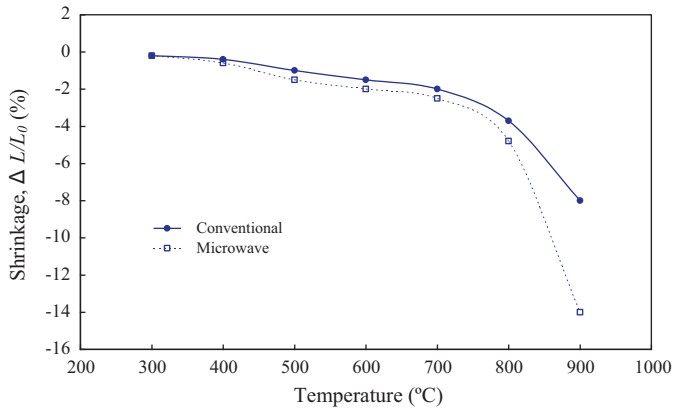


Fig. 2. The shrinkage rate of ZMT ceramics produced by both sintering methods as a function of the temperature.

the conventional process, the density is much lower than those sintered by microwave processing at temperatures  $<880^{\circ}\text{C}$ . The theoretical density of the ZMT ceramic is  $\sim 4.95\text{ g/cm}^3$ .<sup>14</sup> The ZMT ceramics produced by microwave processing can reach over 95% of the theoretical density ( $4.75\text{ g/cm}^3$ ) at  $840^{\circ}\text{C}$ . For conventional processing, the material must be sintered at  $900^{\circ}\text{C}$  to obtain a 95% theoretical density. In other words, the microwave sintering can achieve a high-density ZMT ceramic at a lower heating temperature ( $840^{\circ}\text{C}$ ), while in the conventional sintering, there was no significant densification below  $880^{\circ}\text{C}$ . The microwave sintering temperature was  $60^{\circ}\text{C}$  lower than the conventional sintering. The maximum densities achieved for microwave and conventional sintering were  $4.92\text{ g/cm}^3$  at  $900^{\circ}\text{C}$  and  $4.90\text{ g/cm}^3$  at  $920^{\circ}\text{C}$ , respectively. This clearly indicates that microwave sintering substantially enhanced the densification of ZMT ceramics. The densification effect was evaluated by linear shrinkage ( $\Delta L/L_0$ ) of the samples as shown in Fig. 2. The results show that microwave sintering enhanced the sintering of the samples. It was found that the microwave densification enhancement of ZMT ceramics was temperature-dependent. The microwave heating at  $840^{\circ}\text{C}$  produced the same densification as conventional heating at  $900^{\circ}\text{C}$  ( $60^{\circ}\text{C}$  lower). No significant microwave densification enhancement was observed below  $800^{\circ}\text{C}$ , which indicates significantly accelerated sintering kinetics by microwave processing.

The effect of different sintering modes on the microstructure of ZMT ceramics was observed. SEM micrographs of the fracture surface of the specimens sintered at  $800^{\circ}\text{C}$  are shown in Fig. 3. In Fig. 3(a), it can be seen that the ZMT ceramics produced by conventional processing are rather porous; therefore, the densification of the ceramic is insufficient. For microwave processing, the densification in the sintered specimen is enhanced considerably, as shown in Fig. 3(b). The effect of the microwave processing temperature on the microstructure of ZMT dielectrics was observed. Fig. 4 shows the microstructures of ZMT dielectrics processed for 1 h under different sintering temperatures: (a)  $870^{\circ}\text{C}$ , (b)  $900^{\circ}\text{C}$ , and (c)  $920^{\circ}\text{C}$ . The results indicate that the ZMT dielectric is completely densified at  $870^{\circ}\text{C}$ , as shown in Fig. 4(a). Comparing Fig. 4(a) and (b), the grains of the ZMT ceramics become more obvious at  $900^{\circ}\text{C}$  sintering. It has been reported that  $\text{ZnTiO}_3$  decomposes into  $\text{Zn}_2\text{TiO}_4$  and rutile at approximately  $945^{\circ}\text{C}$ <sup>11,14</sup> and that the ZMT ceramic sintered at  $900^{\circ}\text{C}$  contains two well characterised phases, namely,  $\text{TiO}_2$  and  $\text{ZnTiO}_3$ . It was also reported that the host grains (grey) are of the  $\text{ZnTiO}_3$  phases, and the dark grains are of the rutile phase ( $\text{TiO}_2$ ).<sup>20</sup> The microstructure of the sintered ceramics shows a significant change: the amount of the rutile phase is increased for the samples sintered at  $900$  and  $920^{\circ}\text{C}$ , as shown in Fig. 4(b) and (c), respectively.

### 3.2. Effect of microwave sintering on the Ag diffusion and dielectric properties of ZMT MLCCs

It has been reported that Ag diffusion from the inner electrode occurs during high-temperature cofiring between the ZMT dielectric and the Ag/Pd inner electrode in  $\text{ZnTiO}_3$ -based MLCCs.<sup>21</sup> To understand the diffusion of Ag after cofiring with microwave sintering, an analysis of the Ag element from the central region between the electrodes was carried out. Six positions on the central part were analysed on each sample to ensure WDS reproducibility and reliability. Fig. 5 shows the WDS analysis for Ag diffusion in ZMT MLCCs after different heating processes. When conventional heating is applied, significantly more Ag ions diffused into the dielectric layer. This result is the same as that of our previous study.<sup>19</sup> According to the WDS analysis, the concentration of Ag in the ZMT dielectrics resulting from microwave sintering is below 0.4 at.%,

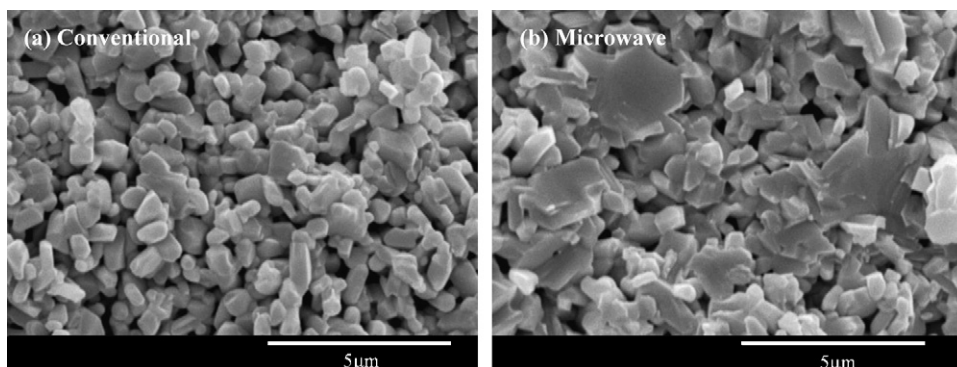


Fig. 3. SEM microstructures for ZMT dielectric sintered at  $800^{\circ}\text{C}$  (a) conventional sintering and (b) microwave sintering.

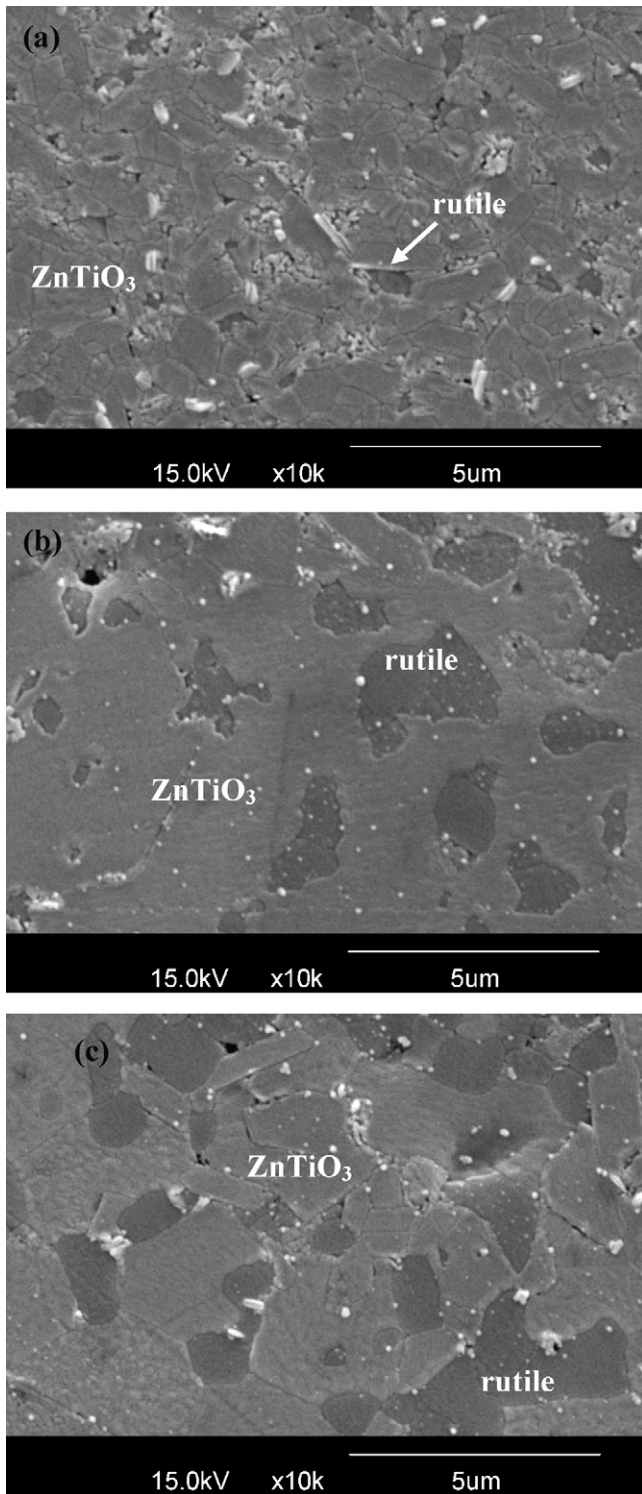


Fig. 4. SEM microstructures for ZMT dielectric with microwave sintering at (a) 870 °C, (b) 900 °C and (c) 920 °C.

whereas that resulting from the diffusion of Ag ions during conventional sintering is approximately 1.0 at.%. This experimental result proves that microwave sintering can effectively prevent the diffusion of Ag ions into the dielectric layer. The reduction of Ag ionic diffusion into the dielectric layer during microwave sintering can be explained by the densification

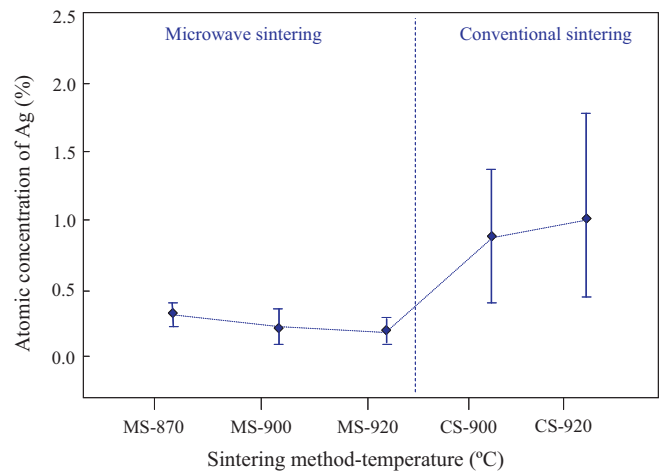


Fig. 5. Average Ag concentration in the dielectric layer of ZMT MLCC with different sintering temperature and method.

of ZMT dielectrics. The microwave sintering process leads to increased densification of the ZMT dielectric during heating (Fig. 1), reducing the porosity of the ZMT dielectric and making it more difficult for Ag to diffuse into the dielectric layer. The microwave electromagnetic energy falls within the frequency range of 300 MHz to 300 GHz. Microwave heating is a process in which the materials couple with the microwaves, absorb the electromagnetic energy volumetrically, and transform into heat. It is different from the conventional process in which heat is transferred between objects by the mechanisms of conduction, radiation and convection.<sup>22,23</sup> When MLCCs are sintered by conventional processing, the ZMT dielectric surface is heated first, and the heat then moves inward. This inward movement means that there is a temperature gradient from the surface to the inside of the dielectric. However, microwave heating generates heat within the material first and then heats the entire volume.<sup>24</sup> This heating mechanism is advantageous for the suppression of Ag diffusion into the ZMT dielectric. The heating mechanism of MLCCs during microwave processing is shown in Fig. 6. For microwave sintering, the microwaves can be absorbed by dielectric materials depending on the value of the dielectric loss factor, but they are reflected by conductors (Ag electrodes). Based on this interaction, the ZMT dielectrics can be expected to be sintered first by microwaves, after which the Ag electrodes will be heated by conduction from the ZMT dielectrics. Therefore, the ZMT dielectrics will be sintered earlier than Ag electrodes. As a result, Ag diffusion into the ZMT dielectric layer becomes more difficult due to high densification of the ZMT dielectric layer. This outcome can be confirmed by examination of a cross-section of the ZMT MLCC. Fig. 7 shows the microstructure of a ZMT MLCC sintered at 900 °C for 1 h under both sintering processes. It can be seen that the Ag electrodes remain completely continuous for microwave sintering as shown in Fig. 7(a). However, Fig. 7(b) shows the microstructure of the ZMT MLCC that underwent conventional sintering, in which it can be seen that the Ag electrodes are discontinuous. The discontinuity of the Ag electrodes may be caused by the diffusion of some Ag ions into the dielectric layer, which agrees with the results in Fig. 5.

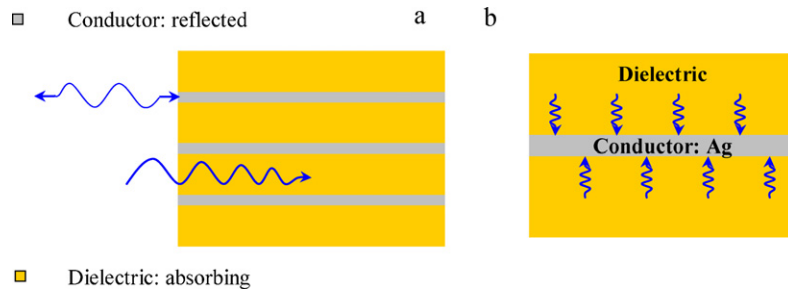


Fig. 6. Mechanism of microwave sintering for multilayer ceramic capacitors: (a) microwave reaction for MLCC and (b) heat conducts to Ag electrode from ZMT dielectric layer.

This result indicates that microwave sintering can effectively prevent the Ag ions from diffusing from the inner electrodes into the dielectric layer. To verify this assertion and understand the prohibition of Ag ion diffusion into the dielectric layer via microwave sintering, the specimen was further analysed using TEM.

TEM analysis was used to investigate the effect of microwave sintering on the Ag ion diffusion. Fig. 8 shows the TEM microstructure and EDX analysis, illustrating the ZMT MLCC sintered at 900 °C via microwave sintering. Fig. 8(a) shows a TEM micrograph of the interface between the electrode and dielectric layer of the ZMT MLCC. The interface between the Ag and the ZMT phases is clear, implying that no interaction occurred at the interface. To understand the extent to which Ag ions diffused into the dielectric ceramics at the grain boundary,

the compositions of the Ag particle and matrix phases are confirmed using EDX analysis as shown in Fig. 8(b) and (c). The EDX analysis for the grain boundary “A” of the ZMT dielectric shows that no Ag ions diffuse into the dielectric layer at the grain boundary as shown in Fig. 8(b). This result indicates that microwave sintering can effectively prevent the diffusion of Ag ions from the inner electrodes into the dielectric layer.

To prove that Ag ion diffusion into the dielectric layer results in the degradation of the insulation resistance (IR) of ZMT MLCCs, they are placed in a constant temperature and humidity environment (85 °C and R.H. 95%) for a long-term IR measurement as shown in Fig. 9. The result indicates that microwave sintering produces a higher IR value. According to a previous study,<sup>19</sup> high Ag ion concentration in the dielectric layer

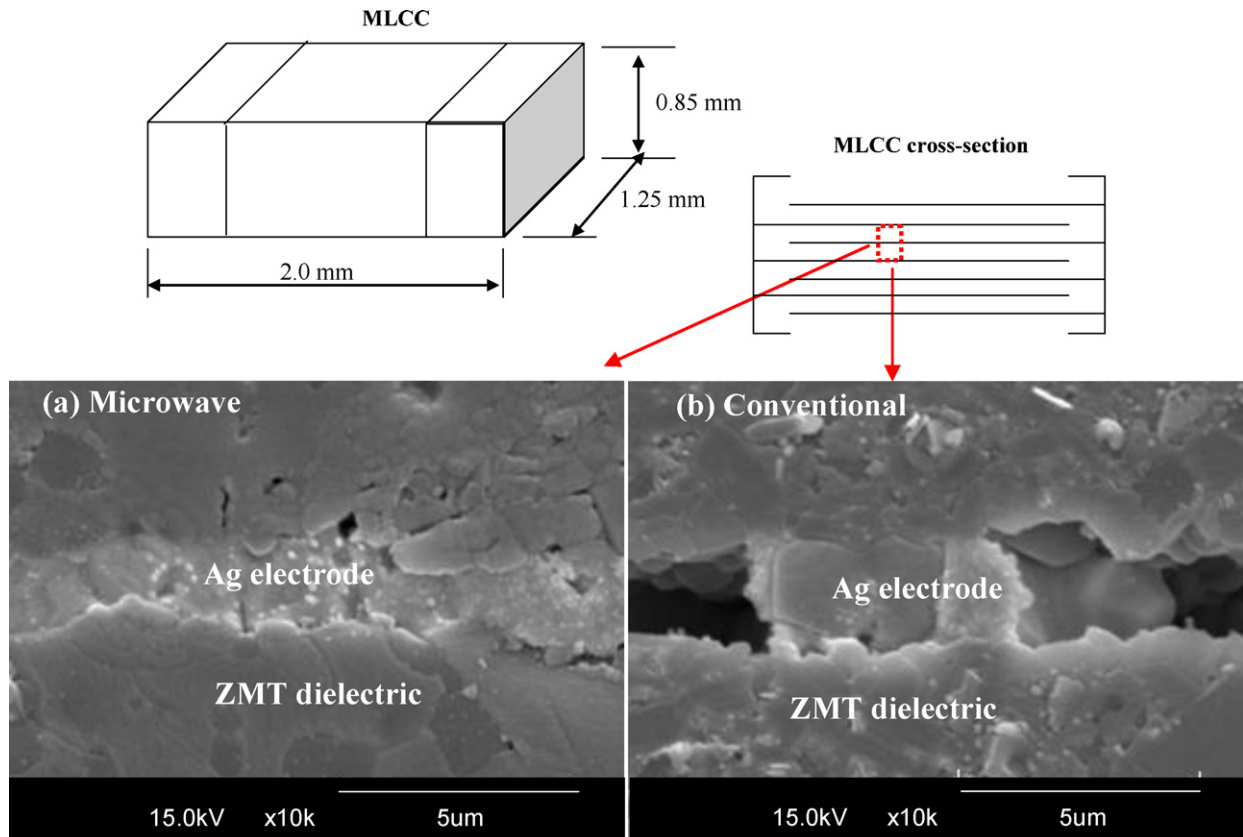


Fig. 7. SEM microstructures illustrating that ZMT MLCC sintered at 900 °C (a) microwave and (b) conventional sintering.

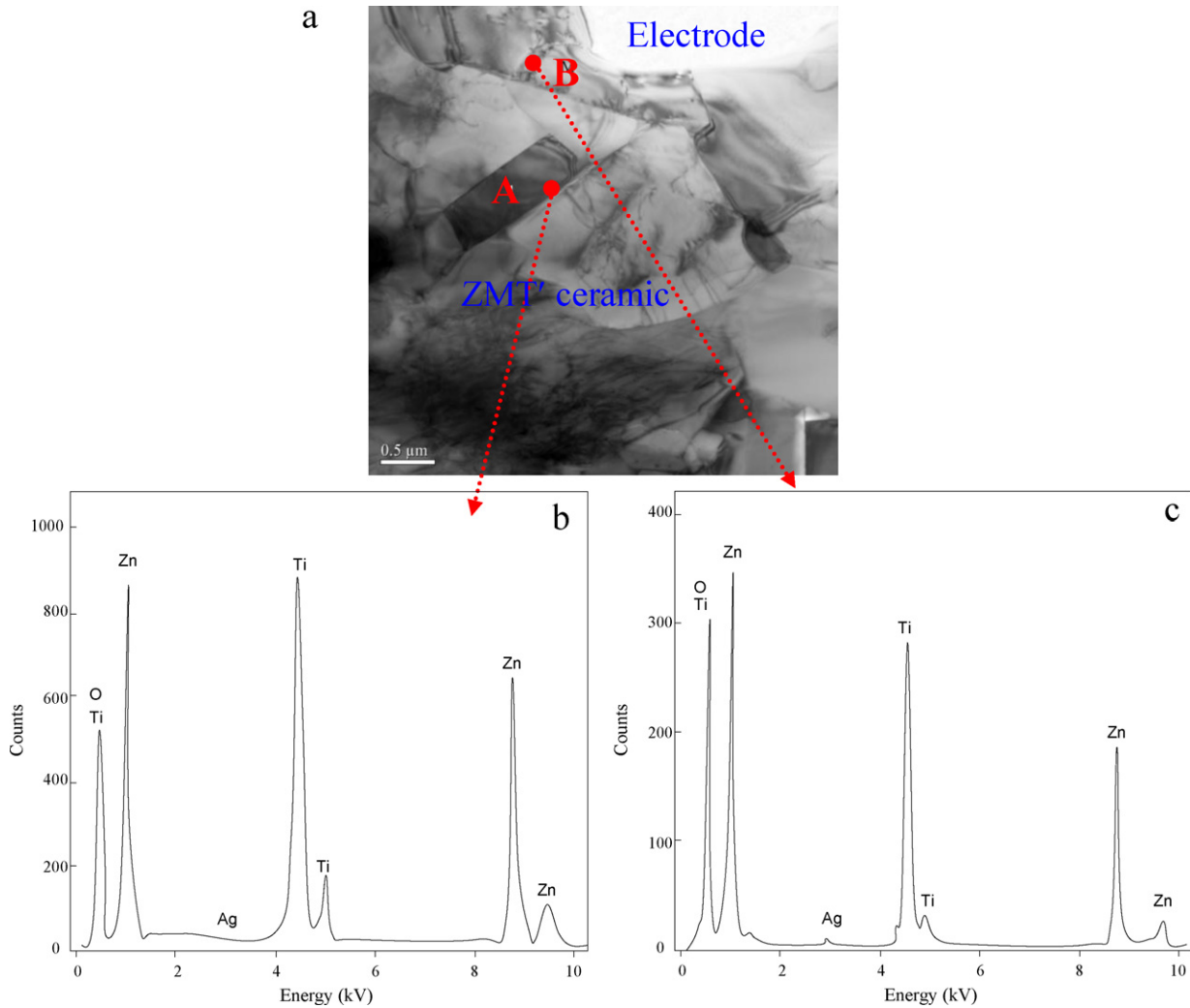


Fig. 8. TEM microstructure of the ZMT MLCC with microwave sintering at 900 °C, where (a) morphology at ZMT dielectric and electrode, (b) EDX composition for grain boundary “A” and (c) EDX composition for grain boundary “B”.

is a known result of conventional sintering. The Ag ions in the dielectric layer of the MLCC can reduce the IR, especially under high temperature and high humidity conditions, which accelerate the decrease of the IR. Therefore, the IR of ZMT MLCCs with microwave sintering is higher than that of ZMT MLCC with conventional sintering. This outcome could be explained by the diffusion of Ag ions into the dielectric layer during cofiring because Ag migration leads to the local intensification of an applied field, which lowers the insulation resistance.<sup>25</sup>

Table 1 shows the electrical properties of ZMT MLCCs with different sintering modes. The microwave sintering temperatures seem to have an effect on the dielectric properties of ZMT

MLCCs because the permittivity ( $\epsilon_r$ ) increases with increasing sinter temperature. In particular, the  $\epsilon_r$  value of ZMT MLCCs sintered at 920 °C is higher than the value for those samples sintered at 900 °C. This result is attributed to the increase in the amount of the rutile phase,<sup>11</sup> as observed in the SEM analysis (Fig. 4). As is well known,<sup>10</sup> the existence of a small amount of the rutile phase can increase the dielectric constant of the ceramic because the dielectric constant of rutile,  $\epsilon_r = 105$ , is much higher than that of the hexagonal  $\text{ZnTiO}_3$  phase,  $\epsilon_r = 19$ . However, some high dielectric loss is observed for MLCCs sintered at 920 °C compared to samples sintered at 900 °C. The breakdown voltage of the ZMT MLCCs is highest for microwave

Table 1  
The electrical properties of ZMT MLCC sintered under different conditions.

Microwave-sintering temperature (°C)	Permittivity	Dielectric loss ( $\times 10^{-4}$ )	Insulation resistance (MOhm)	Breakdown voltage (V/μm)
870	27.1	3.6	45,000	45.7
900	29.9	2.1	250,000	49.3
920	36.0	6.6	380,000	47.1
Conventional	29.0	2.2	150,000	39.7

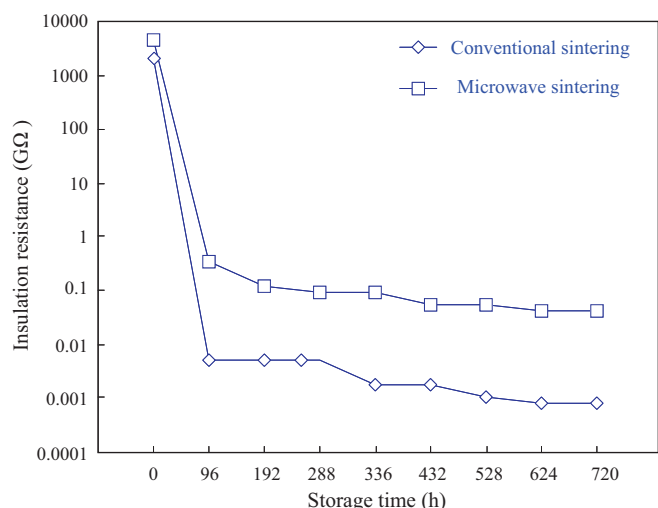


Fig. 9. The electrical resistances measured under a temperature of 85 °C and relative humidity of 95% when ZMT MLCC undergoes different sintering method and storage times.

sintering at 900 °C. In addition, the lowest breakdown voltage (39.7 V/μm) is obtained for conventional sintering. This can be explained by Ag diffusion into the dielectric layer during cofiring because Ag migration leads to a local intensification of an applied field, lowering the breakdown strength. This result can also be confirmed by WDS analysis as shown in Fig. 5 because the concentration of Ag ions for conventional sintering of the ZMT dielectric is higher than that for microwave sintering. In addition, the microwave sintering has been shown to typically enhance the kinetics of densification and grain growth (in some cases).<sup>26</sup> This change in kinetics often leads to differences in microstructure.

#### 4. Conclusion

ZMT MLCCs prepared by different sintering methods were investigated. The results are summarised below.

1. Microwave sintering can achieve a high-density ZMT ceramic at lower heating temperature (840 °C), while in the conventional sintering, there was no significant densification below 880 °C. The microwave sintering temperature was 60 °C lower than the conventional sintering.
2. The effect of microwave sintering on Ag diffusion into the ZMT dielectric was investigated. According to the WDS analysis, the concentration of Ag in the ZMT dielectrics using microwave sintering is below 0.4 at.%, whereas the use of conventional sintering results in an Ag ion concentration of approximately 1.0 at.%. This result indicates that microwave sintering can effectively prevent the Ag ions from the silver electrode from diffusing into the dielectric layer.
3. The ZMT MLCCs with microwave sintering showed increased insulation resistance, which was compared to the results of conventional sintering in a measurement at 85 °C and R.H. 95%. We believe the difference in results is attributable to silver ion diffusion, which may be an

important cause of the degradation of dielectric properties and reliability of MLCCs.

#### Acknowledgement

The authors would like to acknowledge the financial support of this research by the National Science Council of Taiwan under contract No. 99-2221-E-020-018.

#### References

1. Zhou D, Wang H, Yao X, Pang L-X. Microwave dielectric properties of low temperature firing Bi<sub>2</sub>Mo<sub>2</sub>O<sub>9</sub> ceramic. *J Am Ceram Soc* 2008;**91**:3419–22.
2. Kwon D-K, Lanagan MT, Shroud TR. Microwave dielectric properties and low-temperature cofiring of BaTe<sub>4</sub>O<sub>9</sub> with aluminum metal electrode. *J Am Ceram Soc* 2005;**88**:3419–22.
3. Wang XX, Chen WP, Chan HLW, Choy CL. H<sub>2</sub>O-induced degradation in TiO<sub>2</sub>-based ceramic capacitors. *Mater Lett* 2003;**57**:4351–5.
4. Paulsen JL, Reed EK. Highly accelerated lifetesting of base-metal-electrode ceramic chip capacitors. *Microelectron Reliab* 2002;**42**:815–20.
5. Caballero AC, Nieto E, Duran P, Moure C, Kosec M, Samardzija Z, Drazic G. Ceramic-electrode interaction in PZT and PNN-PZT multilayer piezoelectric ceramics with Ag/Pd 70/30 inner electrode. *J Mater Sci* 1997;**32**:3257–62.
6. Zuo RZ, Li LT, Gui ZL. Influence of silver migration on dielectric properties and reliability of relaxor based MLCCs. *Ceram Int* 2000;**26**:673–80.
7. Zuo RZ, Li LT, Zhang NX, Gui ZL. Interfacial reaction of Ag/Pd metals with Pb-based relaxor ferroelectrics including additives. *Ceram Int* 2001;**27**:85–90.
8. Lu CH, Lin JY. Interaction between lead iron niobate/tungstate ceramics and silver/palladium metals. *Ceram Int* 1997;**23**:223–9.
9. Dulin FH, Rase DE. Phase equilibria in the system ZnO–TiO<sub>2</sub>. *J Am Ceram Soc* 1960;**43**:125–9.
10. Kim HT, Nahm S, Byun JD. Low-fired (Zn,Mg)TiO<sub>3</sub> microwave dielectrics. *J Am Ceram Soc* 1999;**82**:3476–81.
11. Kim HT, Kim SH, Nahm S, Byun JD. Low-temperature sintering and microwave dielectric properties of zinc metatitanate–rutile mixtures using boron. *J Am Ceram Soc* 1999;**82**:3043–8.
12. Kim HT, Byun JD, Kim YH. Microstructure and microwave dielectric properties of modified zinc titanates (I). *Mater Res Bull* 1998;**33**:963–70.
13. Fukushima H, Mori H, Hatanaka T, Matsui M. Properties and microstructure of PZT ceramics sintered by microwave. *J Ceram Soc Jpn* 1995;**103**:1011–8.
14. Lee YC, Lee WH, Shiao FT. Microwave dielectric properties of Zn<sub>0.95</sub>Mg<sub>0.05</sub>TiO<sub>3</sub> + 0.25TiO<sub>2</sub> ceramics with 3ZnO–B<sub>2</sub>O<sub>3</sub> addition. *Jpn J Appl Phys* 2004;**43**:7596–600.
15. Haga K, Ishii T, Mashiyama JI, Ikeda T. Dielectric properties of two-phase mixture ceramics composed of rutile and its compounds. *Jpn J Appl Phys* 1992;**31**:3156–61.
16. Halder N, Das Sharma A, Khan SK, Sn A, Maiti HS. Effect of silver addition on the dielectric properties of barium titanate based low temperature processed capacitors. *Mater Res Bull* 1999;**34**:545–50.
17. Zuo RZ, Li LT, Gui ZL, Hung TF, Xu ZK. TEM and EDS investigation of heterogeneous interfaces in cofired multilayer ceramic capacitors. *Mater Sci Eng* 2002;**B95**:1–5.
18. Lee WH, Su CY. Characterization of silver interdiffusion into (Zn,Mg)TiO<sub>3+x</sub>:Bi:Sb multilayer ceramic capacitor. *J Am Ceram Soc* 2007;**90**:2454–9.
19. Lu W-H, Lee Y-C, Tsai P-R. The effect of sintering parameters on silver migration of (Zn,Mg)TiO<sub>3</sub>-based multilayer ceramic capacitor. *Adv Appl Ceram* 2011;**110**:99–107.
20. Lee YC, Lee WH. Effect of glass addition on the microwave dielectric properties of Zn<sub>0.95</sub>Mg<sub>0.05</sub>TiO<sub>3</sub> + 0.25TiO<sub>2</sub> ceramics. *Jpn J Appl Phys* 2005;**44**:1838–43.
21. Lee Y-C. Dielectric properties and reliability of Zn<sub>0.95</sub>Mg<sub>0.05</sub>TiO<sub>3</sub> + 0.25TiO<sub>2</sub> MLCCs with different Pd/Ag ratio of electrodes. *Int J Appl Ceram Technol* 2010;**7**:71–80.

22. Oghbaei M, Mirzaee O. Microwave versus conventional sintering: a review of fundamentals, advantages and applications. *J Alloys Compd* 2010;**494**:175–89.
23. Leonelli C, Veronesi P, Denti L, Gatto A, Iuliano L. Microwave assisted sintering of green metal parts. *J Mater Process Technol* 2008;**205**:489–96.
24. Yadoji P, Peelamedu R, Agrawal D, Roy R. Lower dielectric NiZn ferrites obtained by comparison with conventional sintering. *Mater Sci Eng* 2003;**B98**:269–78.
25. Ruzhong Zuo, Longtu Li, Yin Tang, Zhilun Gui. Characteristics and effects of interfacial interdiffusion in composite multilayer ceramic capacitors. *Mater Chem Phys* 2001;**69**:230–5.
26. Fang Y, Lanagan MT, Agrawal DK, Yang GY, Randall CA, Shrout TR, Henderson A, Randall M, Tajuddin A. An investigation demonstrating the feasibility of microwave sintering of base-metal-electrode multilayer capacitors. *J Electroceram* 2005;**15**:13–9.